

Puerarin alleviates the ototoxicity of gentamicin by inhibiting the mitochondria-dependent apoptosis pathway

PING NIU^{1,2*}, YUXUAN SUN^{3*}, SHIYI WANG⁴, GUANG LI⁴, XIAOMIN TANG³,
JIAQIANG SUN³, CHUNCHEN PAN³ and JINGWU SUN³

¹Department of Otolaryngology-Head and Neck Surgery, Anhui Provincial Hospital, Cheeloo College of Medicine, Shandong University, Jinan, Shandong 250012; ²Department of Otolaryngology, Qingzhou Hospital Affiliated to Shandong First Medical University, Qingzhou People's Hospital, Qingzhou, Shandong 262500; ³Department of Otolaryngology-Head and Neck Surgery, Anhui Provincial Hospital, Hefei, Anhui 230001; ⁴Department of Otolaryngology-Head and Neck Surgery, Affiliated Hospital of Yangzhou University, Yangzhou, Jiangsu 225001, P.R. China

Received February 28, 2021; Accepted September 22, 2021

DOI: 10.3892/mmr.2021.12491

Abstract. Gentamicin (GM) is a commonly used antibiotic, and ototoxicity is one of its side effects. Puerarin (PU) is an isoflavone in kudzu roots that exerts a number of pharmacological effects, including antioxidative and free radical scavenging effects. The present study investigated whether PU could protect against GM-induced ototoxicity in C57BL/6J mice and House Ear Institute-Organ of Corti 1 (HEI-OC1) cells. C57BL/6J mice and HEI-OC1 cells were used to establish models of GM-induced ototoxicity in this study. Auditory brainstem responses were measured to assess hearing thresholds, and microscopy was used to observe the morphology of cochlear hair cells after fluorescent staining. Cell viability was examined with Cell Counting Kit-8 assays. To evaluate cell apoptosis and reactive oxygen species (ROS) production, TUNEL assays, reverse transcription-quantitative PCR, DCFH-DA staining, JC-1 staining and western blotting were performed. PU protected against GM-induced hearing damage in C57BL/6J mice. PU ameliorated the morphological changes of mouse cochlear hair cells and reduced the apoptosis rate of HEI-OC1 cells after GM-mediated damage. GM-induced ototoxicity may be closely related to the upregulation of p53 expression and the activation of endogenous mitochondrial

apoptosis pathways, and PU could protect cochlear hair cells from GM-mediated damage by reducing the production of ROS and inhibiting the mitochondria-dependent apoptosis pathway.

Introduction

Gentamicin (GM) is an aminoglycoside antibiotic that is commonly used in the clinic (1). For more than half a century, despite the advantages of aminoglycosides in terms of their stable properties, broad antibacterial spectrum, strong bactericidal power and low cost, a large number of clinical reports and animal experiments have also proven that aminoglycosides induce ototoxicity (2), which severely limits their clinical application. Current studies have found that the mechanism underlying aminoglycoside ototoxicity may be that aminoglycoside antibiotics can accumulate in cochlear hair cells, and mitochondria are the main site of accumulation (3,4). Moreover, the hair cells located in the basal turn of the basilar membrane have a stronger absorption capacity than those located in the apical turn (5). The damage to cochlear hair cells caused by aminoglycosides is associated with the activity of oxygen radicals, and the expression of caspase-3 is also subsequently increased (6). Thus, GM-induced ototoxicity may be closely related to the overproduction of reactive oxygen species (ROS) in cochlear hair cells and the activation of endogenous mitochondrial apoptosis pathways.

Puerarin (PU) is the main active ingredient among the isoflavones of wild *Pueraria* and dried *Pueraria* (7). Isoflavones are aromatic oxyheterocyclic compounds and effective antioxidants that prevent the formation of oxygen free radicals and exert biological antioxidant effects (8). Based on a number of animal experiments and clinical studies, PU has antioxidant, anti-ageing, anti-inflammatory and anti-osteoporosis activities and is also used to treat hangovers and hypoglycaemia (9,10); in addition, PU is mainly used in the treatment of neurological diseases and cardiovascular diseases (11,12). The mechanism underlying the various pharmacological effects of PU has

Correspondence to: Dr Chunchen Pan or Professor Jingwu Sun, Department of Otolaryngology-Head and Neck Surgery, Anhui Provincial Hospital, 17 Lujiang Road, Hefei, Anhui 230001, P.R. China
E-mail: panchunchen@hotmail.com
E-mail: entsun@ustc.edu.cn

*Contributed equally

Key words: puerarin, gentamicin, ototoxicity, apoptosis, reactive oxygen species, p53

been thoroughly studied and has attracted increasing attention from researchers. PU can improve the learning and memory abilities of ageing mice, and the mechanism underlying its anti-ageing effects is related to the inhibition of mitochondrial dysfunction and the enzyme activity of caspase-3 (13). PU can also significantly improve the activity of superoxide dismutase in ageing mice and enhance its ROS scavenging function. PU may inhibit the expression of caspase-3 and Bax, which are closely related to cell apoptosis, and promote the protein expression of Bcl-2 (11,12). In addition, it has been reported that PU is useful in treating alcoholic liver disease as an antidote and anti-drinking agent (14). However, the effects of PU on GM-induced ototoxicity have not yet been reported.

Apoptosis is a pathophysiological process in which various proteins or factors are involved. p53 is considered to be an important gene that mediates cell apoptosis and plays an important regulatory role in various cellular stress responses (15). The mechanism by which p53 functions is extremely complex, and p53 plays vital roles in the signalling pathways mediated by endogenous regulatory factors. When cells are stimulated by apoptotic signals, the expression of p53 is increased; p53 regulates the expression of Bcl-2 family proteins through transcription-dependent pathways, and p53 can also directly act on mitochondria-mediated apoptosis pathways. In fact, H₂O₂, the most important ROS in redox signalling, has been shown to trigger a typical DNA damage response pathway and the subsequent activation of p53 and apoptosis (16,17). GM-induced ototoxicity may be closely related to the overproduction of ROS in cochlear hair cells, the upregulation of p53 protein expression and the activation of endogenous mitochondrial apoptosis pathways. Thus, in the present study it was hypothesized that PU may protect cochlear hair cells from GM-mediated damage by reducing ROS production and inhibiting the mitochondria-dependent apoptosis pathway.

Materials and methods

Animal experiments and drugs. The animal protocols followed the guidelines of the Institutional Animal Care and Use Committee of University of Science and Technology of China (Jinan, China), and the experiments were conducted in accordance with the National Institutes of Health (NIH) Guide for the Care and Use of Animals in Laboratory Experiments (18). The study was approved by the Institutional Animal Care and Use Committee of University of Science and Technology of China. A total of 24 male C57BL/6J mice (8 days old; 4.5±0.3 g) were purchased from Changzhou Cavens Experimental Animal Co., Ltd. The mice were housed in an SPF facility, where they were under a controlled temperature of 25±2°C, a humidity of 55±5% and a 12-h day/night cycle, and where the mice were allowed to eat and drink *ad libitum*. The health and behaviour of the mice were checked every day. Animals were maintained in accordance with the Guidelines for the Care and Use of Laboratory Animals (18). When the mice were 6 weeks old, the 24 mice were divided into four groups (six mice in each group): The control group; PU group; GM group; and GM + PU group. The mice in the control group were intraperitoneally injected with 1 ml physiological saline once a day for 10 days. The mice in the PU group were intraperitoneally injected with 100 mg/kg PU (Sigma-Aldrich; Merck KGaA)

once a day for 10 days (19). The mice in the GM group were first intraperitoneally injected with 1 ml physiological saline once a day for 3 consecutive days and then intraperitoneally injected with 200 mg/kg GM (Sigma-Aldrich; Merck KGaA) once a day for 7 days (20). The mice in the GM + PU group were first intraperitoneally injected with 100 mg/kg PU once a day for 3 consecutive days and then intraperitoneally injected with 100 mg/kg PU and 200 mg/kg GM once a day for 7 consecutive days. In the entire study, no mice died accidentally. All efforts were made to minimize suffering. All the 24 mice were anaesthetized with an intraperitoneal injection of a combination of ketamine (100 mg/kg) and xylazine (15 mg/kg) (21). At the end of the experiments, the mice were administered with 30% volume displacement rate of CO₂ for euthanasia. Animal death was confirmed by observing cardiac arrest and mydriasis.

Auditory brainstem response (ABR) test. The ABR thresholds of the four groups were measured in the 8th week. The mice were anaesthetized by intraperitoneal injection with a combination of ketamine (100 mg/kg) and xylazine (15 mg/kg) (21), and the mice were kept warm during the ABR recording. ABR measurements were performed by using Tucker-Davis Technology System hardware and software (Tucker-Davis Technologies). The recording electrode was subcutaneously inserted into the tissue at the vertex, and the reference and ground electrodes were subcutaneously placed behind the ears. The ABR was measured with broadband clicks and pure tones at frequencies of 8, 12, 16, 24 and 32 kHz with 1,024 stimulus repetitions per record, and the stimulus sound was decreased from 90 dB SPL to 10 dB SPL successively at 10-dB SPL intervals. When the electrophysiological response to the stimulus sound disappeared, the lowest stimulus sound that triggered a response was defined as the auditory threshold of the mouse tested at this frequency.

Treatment of cochlear basal membranes and staining. After the ABR was detected, the mice were anaesthetized, and perfusion was performed with normal saline and 4% paraformaldehyde. The head was removed, the temporal bone was removed and the cochlea was separated. The cochlea was immersed in a 10% EDTA solution and stored at 4°C for 7 days. The basilar membrane was then isolated from the cochlea under an anatomical microscope. The basilar membrane was fixed in 10% formaldehyde solution at room temperature for 15 min and fluorescence staining was performed with phalloidin (1:100, red) at room temperature in the dark for 30 min. Fluorescence microscopy was used for observation and imaging. The number of outer and inner hair cells in each segment of the basilar membrane was quantified per 100 μm. Images were captured using a fluorescence microscope (Leica Corporation).

Cell culture and treatment. House Ear Institute-Organ of Corti 1 (HEI-OC1) cells were derived from a murine Corti organ; this cell line is a type of auditory cell line and has properties similar to those of hair cells. HEI-OC1 cells were donated by Professor Renjie Chai of Southeast University. HEI-OC1 cells were cultured in high-glucose medium (Gibco; Thermo Fisher Scientific, Inc.) containing 10% foetal bovine

serum (Gibco; Thermo Fisher Scientific, Inc.) in a 10% CO₂ incubator at 33°C. The HEI-OC1 cells in the control group were treated with no drugs. The cells in the GM, PU and H₂O₂ groups were treated with 1.0 mM GM, 100 µg/ml PU and 0.1 mM H₂O₂ for 24 h, respectively. The cells in the GM + PU group were pre-treated with 100 µg/ml PU for 2 h, followed by a combination treatment with 1.0 mM GM for 24 h. The cells in the H₂O₂ + PU group were pre-treated with 100 µg/ml PU for 2 h, followed by a combination treatment with 0.1 mM H₂O₂ for 24 h. All treatments were at 33°C.

Cell viability. HEI-OC1 cells were seeded in a 96-well plate (5,000 cells per well) and incubated overnight at 33°C in 10% CO₂. The cells were treated with different concentrations of GM (0.1, 0.2, 0.5, 1.0 and 2.0 mM) and PU (5, 10, 20, 50, 100, 200 and 300 µg/ml) for 24 h. A total of 10 µl Cell Counting Kit-8 (CCK-8; Sangon Biotech Co., Ltd.) was added to the treated cells in each well and incubated at 37°C for 1 h. The absorbance at 450 nm was determined with an ELISA reader (Multiskan MK3). The cell viability was calculated as (%) (OD assay - OD blank) / (OD control - OD blank) x100%.

Flow cytometry analysis of cell apoptosis. The treated cells were collected and transferred into a centrifuge tube. After centrifugation (1,000 x g, 4°C, 5 min), the cells were resuspended in 100 µl binding buffer. An Annexin V-APC/7-AAD apoptosis kit (BD Biosciences) was used for double staining in the dark. The apoptosis rate of the HEI-OC1 cells was measured by flow cytometry (CytoFLEX S; Beckman Coulter, Inc.). CytExpert (v2.0; Beckman Coulter, Inc.) was used to analyze the data.

Detection of ROS. The intracellular ROS levels were detected by DCFH-DA staining (cat. no. E004; Nanjing Jiancheng Bioengineering Institute). DCFH-DA (10 µM) was added to the treated cells in a 6-well plate, at 1x10⁶ cells per well, and incubated at 33°C in 10% CO₂ for 2 h. The cells were observed and photographed under a fluorescence microscope. Then, ROS production of the HEI-OC1 cells was measured by flow cytometry (Beckman Coulter, Inc.) (22). CytExpert (v2.0; Beckman Coulter, Inc.) was used to analyze the data.

TUNEL assay. A TUNEL assay was used to investigate the morphological characteristics of apoptosis. The treated cells were fixed with 4% paraformaldehyde for 30 min at 20°C. After 20 min of treatment with 0.1% Triton X-100, TUNEL working solution (Beyotime Institute of Biotechnology) was added to the cells for 1 h at 37°C. DAPI staining was performed for 2 min at 20°C. The treated HEI-OC1 cells were then photographed and analyzed under a fluorescence microscope. Images were captured using a fluorescence microscope (Leica Corporation). For each sample, >5 areas were randomly selected for analysis.

Mitochondrial fluorescent probe staining analysis. A JC-1 probe was used to measure mitochondrial depolarization in HEI-OC1 cells. Briefly, cells were treated in 6-well plates, at 1x10⁶ cells per well, as indicated, and then the cells were incubated with an equal volume of JC-1 staining solution (5 µg/ml; Beyotime Institute of Biotechnology) at 37°C for 20 min and

Table I. Primers used in this study.

Gene	Sequences (5'-3')
GAPDH	F: GTATGACTCCACTCACGG R: GGTCTGGCTCCTGGAAGA
Bcl-2	F: ATCGCCCTGTGGATGACTGAGT R: GCCAGGAGAAATCAAACAGAGGC
Bax	F: TCAGGATGCGTCCACCAAGAAG R: TGTGTCCACGGCGGCAATCATC
p53	F: TCCGAAGACTGGATGACTGC R: GATCGTCCATGCAGTGAGGT
Caspase-3	F: GGAAGCGAATCAATGGACTCTGG R: GCATCGACATCTGTACCAGACC

F, forward; R, reverse.

washed twice with PBS. The mitochondrial membrane potentials were monitored by determining the relative amounts of the emissions of mitochondrial JC-1 monomers or aggregates using fluorescence microscopy and flow cytometry. The excitation and emission wavelengths of 514 and 529 nm, respectively, were used to detect the monomeric form of JC-1. JC-1 aggregation was detected at 585 and 590 nm (23). CytExpert (v2.0; Beckman Coulter, Inc.) was used to analyse the data.

RNA extraction and reverse transcription-quantitative PCR (RT-qPCR). RT-qPCR was performed to detect the mRNA expression levels of Bax, caspase-3 and Bcl-2 in the HEI-OC1 cells. Total RNA was isolated from HEI-OC1 cells using RNAiso Plus[®] reagent (Takara Biotechnology Co., Ltd.). Next, according to the product specification, ReverTra-Plus[™] (Toyobo Life Science) was used to reverse transcribe the RNA into cDNA. qPCR was performed using TB Green[®] Premix Ex Taq[™] II (Takara Biotechnology Co., Ltd.). The following thermocycling conditions were used for the qPCR: Initial denaturation at 95°C for 30 sec; followed by 40 cycles at 95°C for 5 sec and 60°C for 34 sec. The primers used in this experiment (24) are shown in Table I. The mRNA expression levels were normalized to GAPDH expression, and gene expression was calculated by using the 2^{-ΔΔC_q} method in this study (25).

Western blotting. HEI-OC1 cells were lysed in RIPA buffer (Wuhan Servicebio Technology Co., Ltd.) or Cell Mitochondria Isolation kit (Beyotime Institute of Biotechnology). The total protein content was determined using a BCA Protein assay kit (Beyotime Institute of Biotechnology). Protein samples (20 µg) were resolved by 10% SDS-PAGE (Wuhan Servicebio Technology Co., Ltd.), and subsequently transferred to polyvinylidene fluoride membranes (MilliporeSigma). The membranes were blocked with 5% skimmed milk (P0216; Beyotime Institute of Biotechnology) for 1 h at room temperature. Then, the proteins were incubated with primary antibodies overnight in a 4°C refrigerator, followed by incubation with secondary antibodies [HRP-conjugated Affinipure Goat Anti-Rabbit IgG(H+L); cat. no. SA00001-2; 1:5,000,

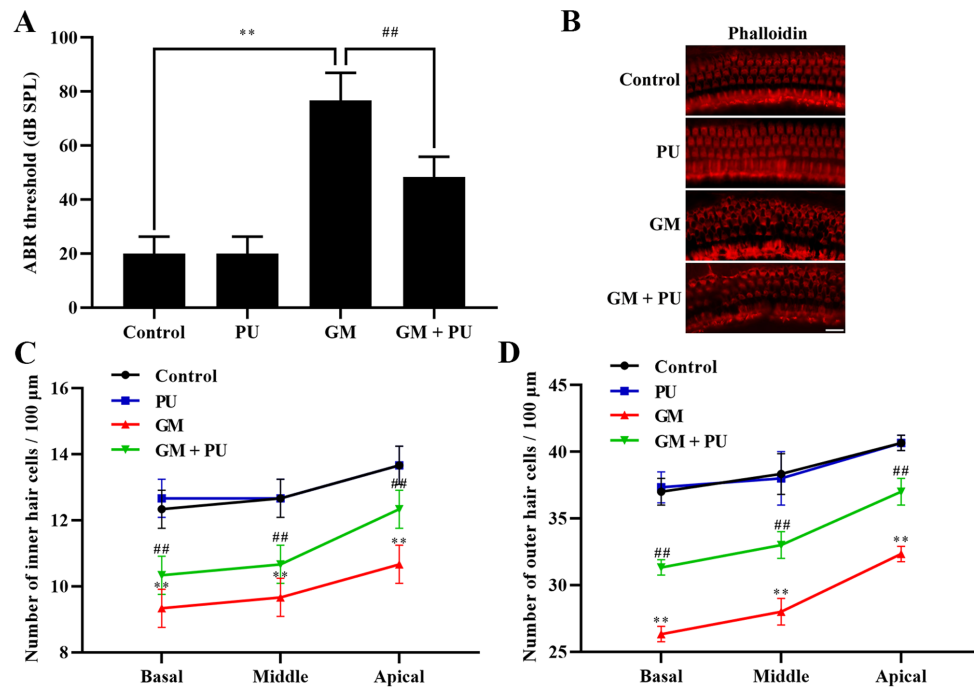


Figure 1. Effects of PU and GM in C57BL/6J mice. (A) Statistical analysis of ABR threshold. $n=6$. ** $P<0.01$ GM group vs. control group; ## $P<0.01$ GM + PU group vs. GM group. (B) Image of basilar membrane stained with phalloidin. Scale bar, 20 μm . (C and D) Statistical analysis of the surviving outer and inner hair cells in the four groups. $n=6$. ** $P<0.01$ GM group vs. control group; ## $P<0.01$ GM + PU group vs. GM group. PU, puerarin; GM, gentamicin; ABR, auditory brainstem response.

ProteinTech Group, Inc.] at room temperature for 1 h. An ECL kit (Wuhan Servicebio Technology Co., Ltd.) was used to detect the immunoreactive bands. Protein expression was detected using a Clinx ChemiScope 3300 (Clinx, Inc.). ImageJ software (v1.8; National Institutes of Health, Inc.) was used to quantify protein expression levels. GAPDH (cat. no. 5174; 1:1,000; Cell Signaling Technology, Inc.) and Cox IV (cat. no. 4850; 1:1,000; Cell Signaling Technology, Inc.) (26) were used as the loading controls. The primary antibodies used were specific for p53 (cat. no. 2524; 1:1,000; Cell Signaling Technology, Inc.), Bcl-2 (cat. no. sc-7382; 1:1,000; Santa Cruz Biotechnology, Inc.), cleaved-caspase-3 (cat. no. 9661; 1:1,000; Cell Signaling Technology, Inc.), caspase-3 (cat. no. 14220; 1:1,000; Cell Signaling Technology, Inc.), Bax (cat. no. 2772; 1:1,000; Cell Signaling Technology, Inc.) and cytochrome *c* (Cyto C; cat. no. 11940; 1:1,000; Cell Signaling Technology, Inc.).

Statistical analysis. The statistical software GraphPad Prism 7 (GraphPad Software, Inc.) was used to analyse the significance of the data. All experimental results were independently repeated at least three times. All the data were collected from six or more samples in each of the experimental groups. The data are expressed as the mean \pm standard error of the mean, and one-way ANOVA followed by Tukey's post hoc test was performed. $P<0.05$ was considered to indicate a statistically significant difference.

Results

PU protects against GM-induced hearing loss in C57BL/6J mice. The ABR threshold recording results showed that there was no difference between the PU and control groups. The

threshold value of the GM group was significantly increased, with an increasing trend within the frequency range of 4 to 32 kHz, and the increase was more obvious at high frequencies (Fig. 1A). The threshold value of the GM + PU group was lower than that of the GM group.

PU attenuates GM-induced cochlear hair cell damage. The basal membrane of the cochlea and hair cells were stained with phalloidin (Fig. 1B). The results showed that the hair cells in the Control and PU groups were closely and neatly arranged. In the GM group, the hair cells were disorganized and partially absent, and the cilia were prostrate. Furthermore, the damage to hair cells in the basal and middle turns was more serious than that in the apical turn (Fig. 1C and D). The degree of hair cell damage in the GM + PU group was lower than that in the GM group.

PU improves the survival rate of HEI-OC1 cells treated with GM. CCK-8 assays were used to detect the viability of HEI-OC1 cells (Fig. 2). The results showed that the viability of the HEI-OC1 cells treated with 1 mM GM was $\sim 50\%$ (Fig. 2A). The HEI-OC1 cell viability was not affected by treatment with 5, 10, 20, 50 or 100 $\mu\text{g}/\text{ml}$ PU, while 200 and 300 $\mu\text{g}/\text{ml}$ PU decreased the viability of the HEI-OC1 cells (Fig. 2B). HEI-OC1 cells were pre-treated with different concentrations of PU (10, 50, 100 and 200 $\mu\text{g}/\text{ml}$) for 2 h, followed by a combination treatment with 1.0 mM GM for 24 h. It was demonstrated that the viability of the cells treated with 100 $\mu\text{g}/\text{ml}$ PU was the highest (Fig. 2C). Based on these results, treatment with 1 mM GM for 24 h was considered to be the appropriate condition for the HEI-OC1 cell damage model, and 100 $\mu\text{g}/\text{ml}$ PU was the optimal concentration for protecting HEI-OC1 cells from

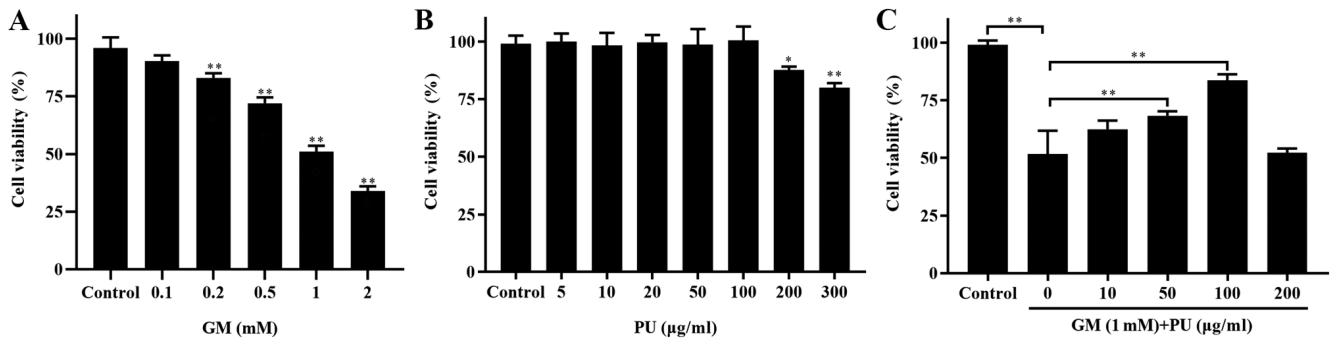


Figure 2. Effects of PU and GM in HEI-OC1 cells as determined via Cell Counting Kit-8 assays. (A) Viability of HEI-OC1 cells treated with different concentrations of GM for 24 h. n=6. **P<0.01. (B) Effect of PU on HEI-OC1 cell viability. Cells were treated with various concentrations of PU for 24 h. n=6. *P<0.05, **P<0.01. (C) Cells were pre-treated with various doses of PU for 2 h prior to the addition of 1 mM gentamicin and further cultured for 24 h. n=6. **P<0.01. PU, puerarin; GM, gentamicin; HEI-OC1, House Ear Institute-Organ of Corti I.

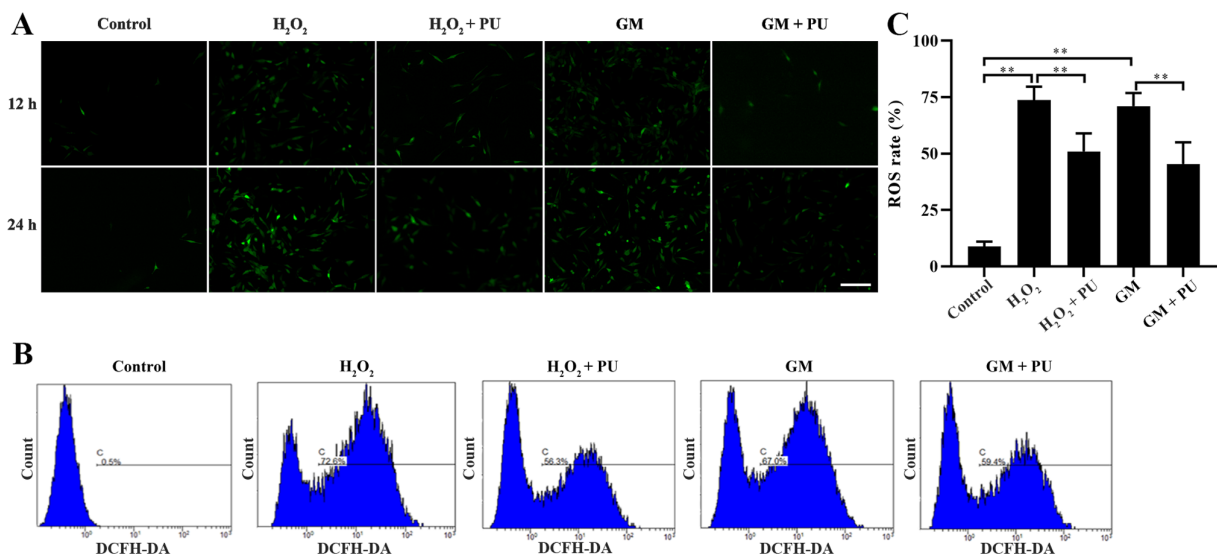


Figure 3. Effects of PU and GM on ROS in HEI-OC1 cells as determined by staining with DCFH-DA. (A) Image of HEI-OC1 cells stained with DCFH-DA (green). The treated cells were observed under a fluorescence microscope. Scale bar, 100 μ m. (B) The fluorescence of DCFH-DA was detected to determine the levels of ROS in the cells by flow cytometry. (C) The ratios of ROS-positive cells and ROS-negative cells were statistically analysed. n=6. **P<0.01. PU, puerarin; GM, gentamicin; HEI-OC1, House Ear Institute-Organ of Corti I; ROS, reactive oxygen species.

GM-mediated damage. Therefore, the aforementioned treatment conditions were selected for subsequent cell experiments.

PU attenuates GM-induced oxidative stress in HEI-OC1 cells. The cells in the Control, H₂O₂, H₂O₂ + PU, GM and GM + PU groups were stained with fluorescent DCFH-DA for 12 and 24 h, according to the manufacturer's instructions, and the cells were photographed under a fluorescence microscope (Fig. 3A). ROS were detected by DCFH-DA, and the intensity of green fluorescence was proportional to the level of ROS in the cells. The results indicated that the amount of intracellular ROS in the H₂O₂ and GM groups were notably increased in the 24 h staining group compared with the 12 h staining group, and PU could reduce the amount of intracellular ROS production induced by H₂O₂ and GM. Flow cytometry was used to detect the green fluorescence intensity of DCFH-DA in the cells after 24 h of treatment in each group (Fig. 3B). The statistical results also showed that PU could significantly reduce the ROS levels in the HEI-OC1 cells after treatment with H₂O₂ and GM (Fig. 3C).

PU attenuates GM-induced damage to mitochondrial membrane in HEI-OC1 cells. JC-1 could aggregate in normal mitochondria and emit red fluorescence. The exposure of HEI-OC1 cells to GM (1 mM) for 24 h resulted in the dissipation of the $\Delta\Psi_m$, which was shown by increased green fluorescence and decreased red fluorescence after JC-1 staining. Pre-treatment with PU (100 μ M) moderated this dissipation, indicating the protective effect of PU (Fig. 4A). The mitochondrial membrane potential of each group was evaluated with JC-1 stain by flow cytometry. Cells in the GM group displayed a lower ratio of mitochondria with normal potential. Pre-treatment of the cells with PU displayed a higher ratio (Fig. 4B and C). The western blotting results suggested that the Cyto C expression levels were significantly reduced in the mitochondria in the GM group compared with the Control group, but increased in the cytoplasm in the GM group. These changes were reversed following pre-treatment with PU (Fig. 4D and E).

PU inhibits the GM-induced apoptosis of HEI-OC1 cells. The apoptosis of HEI-OC1 cells in each group was detected via

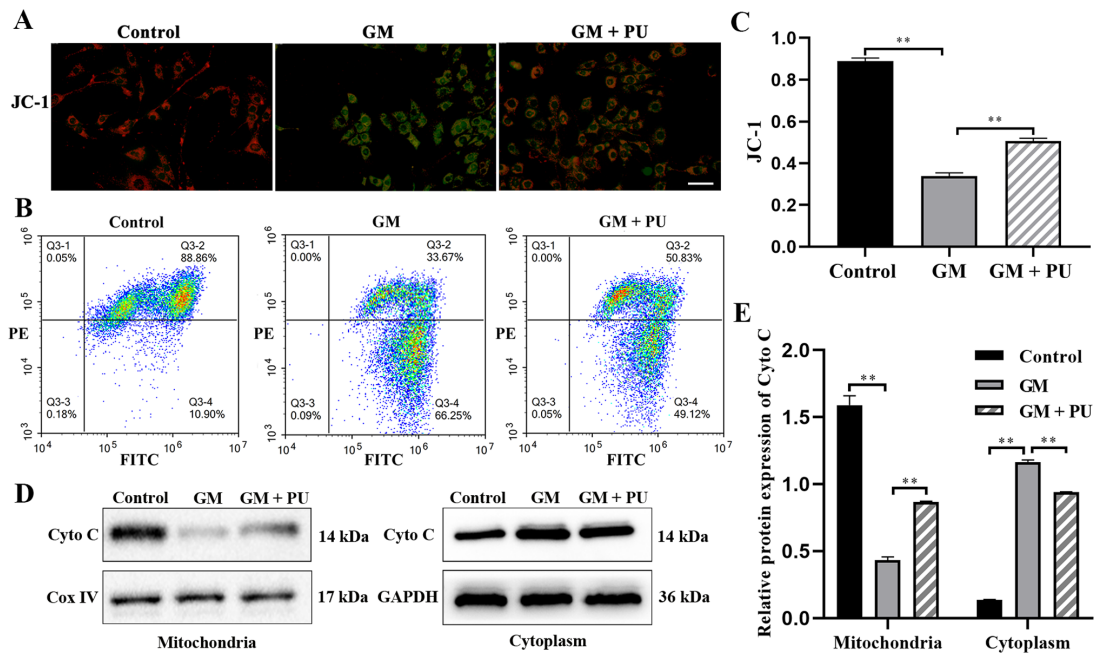


Figure 4. Effect of PU on the GM-induced permeability of the mitochondrial membrane in HEI-OC1 cells. Red fluorescence represents the mitochondrial aggregated form of JC-1, indicating intact mitochondrial membrane potential. Green fluorescence represents the monomeric form of JC-1, indicating dissipation of the $\Delta\Psi_m$. (A) Representative photographs of JC-1 staining in different groups. Scale bar, 200 μm . (B) Flow cytometry study of the mitochondrial membrane potential. (C) Mitochondrial membrane potential analysis. $n=6$. $**P<0.01$. (D) Expression of Cyto C in the mitochondria and cytoplasm of HEI-OC1 cells as determined by western blotting. (E) Statistical analysis of protein expression in each group. $n=6$. $**P<0.01$. PU, puerarin; GM, gentamicin; HEI-OC1, House Ear Institute-Organ of Corti 1; Cyto C, cytochrome *c*.

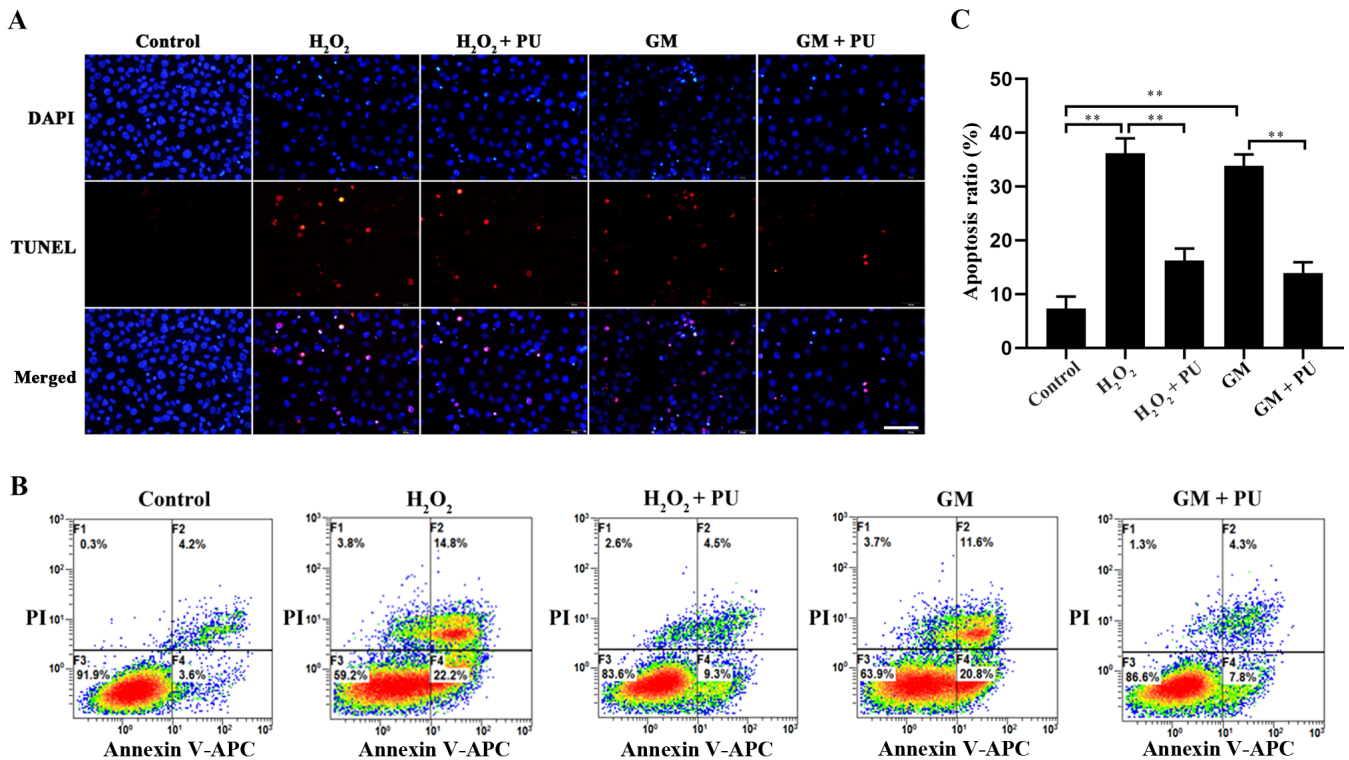


Figure 5. Rate of apoptosis after different treatments as determined by TUNEL assay and flow cytometry. (A) Image of HEI-OC1 cells stained with TUNEL staining. Nuclei were stained with DAPI (blue) and HEI-OC1 cells were stained with TUNEL (red). Scale bar, 100 μm . (B) Flow cytometry was used to assess apoptosis after treatment under different conditions for 24 h. (C) The apoptotic rate of the cells was statistically analysed. $n=6$. $**P<0.01$. PU, puerarin; GM, gentamicin; HEI-OC1, House Ear Institute-Organ of Corti 1.

the TUNEL method (Fig. 5A) and flow cytometry (Fig. 5B). The results showed that apoptosis was significantly increased

after H₂O₂ and GM treatment and that PU pre-treatment significantly reduced this apoptosis (Fig. 5C). The RT-qPCR

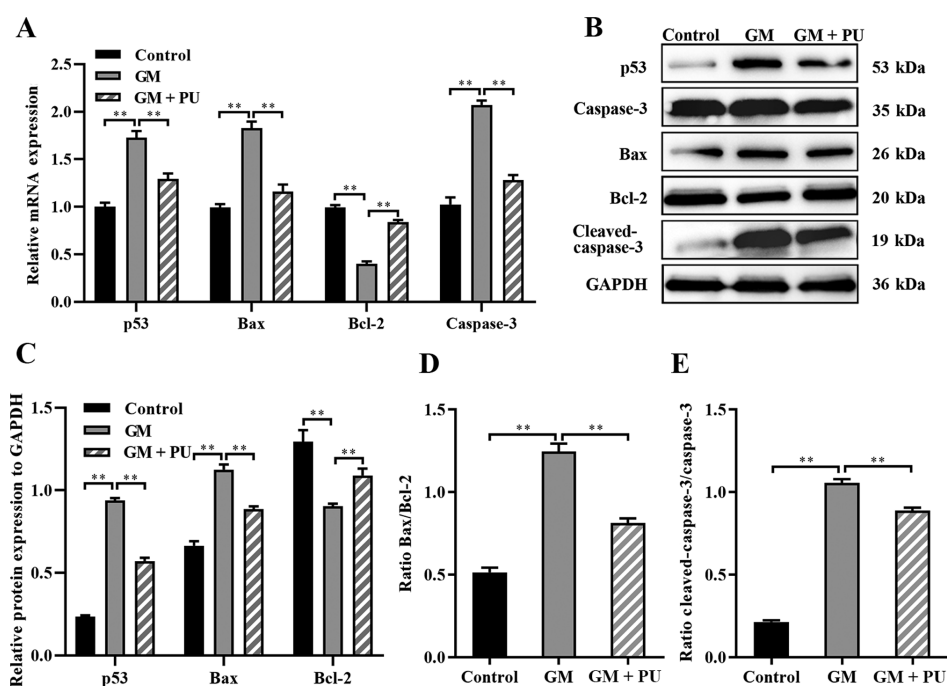


Figure 6. Expression levels of caspase-3, cleaved-caspase-3, Bcl-2, Bax and p53 were analysed via RT-qPCR and western blotting. (A) The mRNA expression levels of caspase-3, Bcl-2, Bax and p53 in each group were detected by RT-qPCR. n=6. **P<0.01. (B) The relative expression levels of p53, caspase-3, Bax, Bcl-2 and cleaved-caspase-3 were analysed via western blotting. (C) Statistical analysis of protein expression in each group. n=6. **P<0.01. (D) The Bax to Bcl-2 ratio. Statistical analysis of protein expression n=6. **P<0.01. (E) The cleaved-caspase-3 to caspase-3 ratio. Statistical analysis of protein expression. n=6. **P<0.01. PU, puerarin; GM, gentamicin; RT-qPCR, reverse transcription-quantitative PCR.

results suggested that compared with the GM group, the GM + PU group exhibited significantly reduced mRNA expression of Bax, caspase-3 and p53, and increased mRNA expression of Bcl-2 (Fig. 6A). The western blotting results (Fig. 6B) showed that p53 expression was increased after the HEI-OC1 cells were treated with GM; moreover, PU could decrease the GM-induced expression of p53. Compared with that in the GM group, the Bax and cleaved-caspase-3 expression in the GM + PU group was significantly decreased, while the Bcl-2 expression was increased (Fig. 6C). Moreover, the Bax/Bcl-2 ratio and cleaved-caspase-3/caspase-3 ratio in the GM + PU group was significantly lower than that in the GM group (Fig. 6D and E).

Discussion

PU is mainly used in the treatment of neurological diseases, cardiovascular diseases and hepatic impairment (7). In the present study, it was found that PU could protect the hearing of GM-treated C57BL/6J mice. We will build more samples and conduct further animal experiments based on this mouse model in follow-up studies. The HEI-OC1 cell line is extremely sensitive to ototoxic drugs. Moreover, the HEI-OC1 cell line is a very useful cell model that has been widely used in a number of studies investigating the molecular mechanism underlying ototoxicity and in studies that screen novel drugs with protective effects *in vitro* (27,28). After treatment with high concentrations of PU, cell viability was decreased. This finding indicated the potential toxicity of high concentrations of PU. We will conduct further in-depth research on this toxicity in the future.

The main sites of aminoglycoside aggregation in cochlear hair cells are the mitochondria, which are the main organelles

that produce oxygen free radicals (29). Appropriate ROS levels can promote immunity, repair and growth of the body, but excessive ROS levels can cause damage to mitochondria and lead to programmed cell death (30). ROS include H_2O_2 , OH^- , NO and ONOO $^-$. Among these ROS, H_2O_2 easily penetrates the plasma membrane and produces the highly reactive free radical OH^- , which leads to damage to cells and tissues and induces cell apoptosis. H_2O_2 has been widely used to establish *in vitro* models of oxidative stress damage (31). In the present study, H_2O_2 was used to establish a control group for oxidative stress injury.

Although the mechanism underlying GM-induced injury has not been determined, ROS may be key players in this mechanism (32), and ROS can also cause oxidative stress and cell damage. The ototoxicity induced by GM is related to the production of ROS, which leads to damage to the auditory hair cells in Corti organs. For a long time, cochlear sensory cells have been known to produce ROS after exposure to aminoglycoside compounds (33). p53 is an important protein that mediates cell apoptosis, and p53 is directly regulated by redox signals due to its readily oxidized cysteine (16). Previous studies have shown that p53 is activated when ROS levels increase (16,34). Moreover, p53 expression has been demonstrated to be positively correlated with Bax expression (35). Bax not only antagonizes the inhibitory effect of Bcl-2 on apoptosis, but also promotes apoptosis. Caspase-3 is a regulator of cell death and plays an important role in the progression of apoptosis. Caspase-3 is a protease that directly leads to the disintegration of apoptotic cells and plays a central role in the network of apoptotic mechanisms. As an upstream protein that regulates caspase-3, Bax can activate caspase-3 and initiate the caspase cascade (36). The cytotoxicity of GM

in hair cells is mainly due to the initiation of the mitochondrial apoptosis pathway (29). In the present study, p53 expression was increased, and p53 regulated the expression of Bcl-2 family proteins when ROS accumulated in HEI-OC1 cells. Bax and Bcl-2 form heteropolymers, enhance mitochondrial membrane permeability, release apoptotic factors into the cytoplasm and stimulate the caspase apoptotic pathway, leading to the programmed death of HEI-OC1 cells (11). Investigation into the regulatory roles of ROS and p53 was not performed in the present study, so these results may have limited generalizability. In future studies, p53 and ROS inhibitors will be used to clarify the protective effect of ROS and p53 on PU in auditory hair cell damage induced by GM.

Previous studies have shown that PU has a variety of pharmacological activities and exerts antioxidant effects (11,37). The present study found that PU protected against GM-induced hearing damage in C57BL/6J mice and ameliorated the morphological changes in mouse cochlear hair cells after GM-mediated damage. It was also observed that PU could reduce the production of ROS, downregulate the expression of p53, Bax and caspase-3, and upregulate the expression of Bcl-2 in GM- and H₂O₂-treated HEI-OC1 cells. After treatment of HEI-OC1 cells with GM and H₂O₂, the expression of p53 was significantly increased. It was demonstrated that PU may ameliorate GM-induced ototoxicity, which is at least partially mediated by p53-regulated apoptotic signalling pathways, by inhibiting the mitochondria-dependent apoptosis pathway. This study provided novel insights into potential therapeutic targets for protecting against GM-induced ototoxicity. PU could be used as a protective agent against the ototoxicity caused by GM.

Acknowledgements

The authors would like to thank Dr Panpan Huang, Dr Wenxiang Fang and Dr Guodong Shen from the University of Science and Technology of China (Hefei, China), for their technical assistance. This work was supported by Anhui Provincial Key Laboratory of Tumor Immunotherapy and Nutrition Therapy (Hefei, China), which provided experimental equipment.

Funding

This research was supported by the National Natural Sciences Foundation of China (grant nos. 81800911 and 81470699), the Anhui Natural Science Foundation (grant no. 1808085QH248) and Fundamental Research Funds for the Central Universities (grant no. WK9110000053).

Availability of data and materials

The datasets used and/or analysed during the current study are available from the corresponding author on reasonable request.

Authors' contributions

PN and YS contributed equally to the work and should be regarded as co-first authors. CP and Jing S conceived and

designed the study. PN, YS, SW, GL, XT and Jia S performed the cell and animal experiments. PN and YS performed the statistical analysis and drafted the manuscript. CP reviewed and edited the manuscript. PN and CP confirm the authenticity of all the raw data. All the authors read and approved the final manuscript.

Ethics approval and consent to participate

The animal protocols followed the guidelines of the Institutional Animal Care and Use Committee of University of Science and Technology of China (Jinan, China), and the experiments were conducted in accordance with the National Institutes of Health (NIH) Guide for the Care and Use of Animals in Laboratory Experiments. The study was approved by the Institutional Animal Care and Use Committee of University of Science and Technology of China [approval no. 2020-N(A)-032]. Anhui Provincial Hospital is the other name for the First Affiliated Hospital of the University of Science and Technology of China.

Patient consent for publication

Not applicable.

Competing interests

The authors declare that they have no competing interests.

References

- Liu J, Kachelmeier A, Dai C, Li H and Steyger PS: Uptake of fluorescent gentamicin by peripheral vestibular cells after systemic administration. *PLoS One* 10: e0120612, 2015.
- Ding D, Zhang J, Jiang H, Xuan W, Qi W and Salvi R: Some Ototoxic Drugs Destroy Cochlear Support Cells Before Damaging Sensory Hair Cells. *Neurotox Res* 37: 743-752, 2020.
- Yao L, Zhang JW, Chen B, Cai M, Feng D, Wang Q, Wang X, Sun J, Zheng Y, Wang G and Zhou F: Mechanisms and pharmacokinetic/pharmacodynamic profiles underlying the low nephrotoxicity and ototoxicity of etimicin. *Acta Pharmacol Sin* 41: 866-878, 2020.
- Kros CJ and Steyger PS: Aminoglycoside- and Cisplatin-Induced Ototoxicity: Mechanisms and Otoprotective Strategies. *Cold Spring Harb Perspect Med* 9: a033548, 2019.
- Liu Y, Yu Y, Chu H, Bing D, Wang S, Zhou L, Chen J, Chen Q, Pan C, Sun Y, *et al*: 17-DMAG induces Hsp70 and protects the auditory hair cells from kanamycin ototoxicity in vitro. *Neurosci Lett* 588: 72-77, 2015.
- Yang Q, Zhou Y, Yin H, Li H, Zhou M, Sun G, Cao Z, Man R, Wang H and Li J: PINK1 Protects Against Gentamicin-Induced Sensory Hair Cell Damage: Possible Relation to Induction of Autophagy and Inhibition of p53 Signal Pathway. *Front Mol Neurosci* 11: 403, 2018.
- Mahdy HM, Mohamed MR, Emam MA, Karim AM, Abdel-Naim AB and Khalifa AE: The anti-apoptotic and anti-inflammatory properties of puerarin attenuate 3-nitropropionic-acid induced neurotoxicity in rats. *Can J Physiol Pharmacol* 92: 252-258, 2014.
- Umeno A, Horie M, Murotomi K, Nakajima Y and Yoshida Y: Antioxidative and Antidiabetic Effects of Natural Polyphenols and Isoflavones. *Molecules* 21: 708, 2016.
- Xiong FL, Sun XH, Gan L, Yang XL and Xu HB: Puerarin protects rat pancreatic islets from damage by hydrogen peroxide. *Eur J Pharmacol* 529: 1-7, 2006.
- Kim J, Kim KM, Kim CS, Sohn E, Lee YM, Jo K and Kim JS: Puerarin inhibits the retinal pericyte apoptosis induced by advanced glycation end products in vitro and in vivo by inhibiting NADPH oxidase-related oxidative stress. *Free Radic Biol Med* 53: 357-365, 2012.

11. Zhang Y, Yang X, Ge X and Zhang F: Puerarin attenuates neurological deficits via Bcl-2/Bax/cleaved caspase-3 and Sirt3/SOD2 apoptotic pathways in subarachnoid hemorrhage mice. *Biomed Pharmacother* 109: 726-733, 2019.
12. Liu B, Zhao C, Li H, Chen X, Ding Y and Xu S: Puerarin protects against heart failure induced by pressure overload through mitigation of ferroptosis. *Biochem Biophys Res Commun* 497: 233-240, 2018.
13. Liu S, Cao XL, Liu GQ, Zhou T, Yang XL and Ma BX: The in silico and in vivo evaluation of puerarin against Alzheimer's disease. *Food Funct* 10: 799-813, 2019.
14. Liu YS, Yuan MH, Zhang CY, Liu HM, Liu JR, Wei AL, Ye Q, Zeng B, Li MF, Guo YP, *et al*: Puerariae Lobatae radix flavonoids and puerarin alleviate alcoholic liver injury in zebrafish by regulating alcohol and lipid metabolism. *Biomed Pharmacother* 134: 111121, 2021.
15. He L, Chen Y, Feng J, Sun W, Li S, Ou M and Tang L: Cellular senescence regulated by SWI/SNF complex subunits through p53/p21 and p16/pRB pathway. *Int J Biochem Cell Biol* 90: 29-37, 2017.
16. Shi T and Dansen TB: Reactive Oxygen Species Induced p53 Activation: DNA Damage, Redox Signaling, or Both? *Antioxid Redox Signal* 33: 839-859, 2020.
17. Valverde M, Lozano-Salgado J, Fortini P, Rodriguez-Sastre MA, Rojas E and Dogliotti E: Hydrogen Peroxide-Induced DNA Damage and Repair through the Differentiation of Human Adipose-Derived Mesenchymal Stem Cells. *Stem Cells Int* 2018: 1615497, 2018.
18. National Research Council: Guide for the Care and Use of Laboratory Animals. National Academies Press, Washington, DC, 2010. <https://www.ncbi.nlm.nih.gov/books/NBK54050/>.
19. Chen X, Qian L, Wang B, Zhang Z, Liu H, Zhang Y and Liu J: Synergistic Hypoglycemic Effects of Pumpkin Polysaccharides and Puerarin on Type II Diabetes Mellitus Mice. *Molecules* 24: 955, 2019.
20. Zhang X and Yu J: Baicalin attenuates gentamicin-induced cochlear hair cell ototoxicity. *J Appl Toxicol* 39: 1208-1214, 2019.
21. Svorc P Jr, Bačová I, Svorc P and Bužga M: Autonomic nervous system under ketamine/ xylazine and pentobarbital anaesthesia in a Wistar rat model: a chronobiological view. *Prague Med Rep* 114: 72-80, 2013.
22. Eruslanov E and Kusmartsev S: Identification of ROS using oxidized DCFDA and flow-cytometry. *Methods Mol Biol* 594: 57-72, 2010.
23. Lin H, Xiong H, Su Z, Pang J, Lai L, Zhang H, Jian B, Zhang W and Zheng Y: Inhibition of DRP-1-Dependent Mitophagy Promotes Cochlea Hair Cell Senescence and Exacerbates Age-Related Hearing Loss. *Front Cell Neurosci* 13: 550, 2019.
24. Yu X, Liu W, Fan Z, Qian F, Zhang D, Han Y, Xu L, Sun G, Qi J, Zhang S, *et al*: c-Myb knockdown increases the neomycin-induced damage to hair-cell-like HEI-OC1 cells in vitro. *Sci Rep* 7: 41094, 2017.
25. Livak KJ and Schmittgen TD: Analysis of relative gene expression data using real-time quantitative PCR and the 2(-Delta Delta C(T)) Method. *Methods* 25: 402-408, 2001.
26. Stevens JM: Cytochrome *c* as an experimental model protein. *Metallomics* 3: 319-322, 2011.
27. Kalinec G, Thein P, Park C and Kalinec F: HEI-OC1 cells as a model for investigating drug cytotoxicity. *Hear Res* 335: 105-117, 2016.
28. Park C, Thein P, Kalinec G and Kalinec F: HEI-OC1 cells as a model for investigating prestin function. *Hear Res* 335: 9-17, 2016.
29. Kros CJ and Steyger PS: Aminoglycoside- and Cisplatin-Induced Ototoxicity: Mechanisms and Otoprotective Strategies. *Cold Spring Harb Perspect Med* 9: a033548, 2019.
30. Circu ML and Aw TY: Reactive oxygen species, cellular redox systems, and apoptosis. *Free Radic Biol Med* 48: 749-762, 2010.
31. Wang Z, Wei D and Xiao H: Methods of cellular senescence induction using oxidative stress. *Methods Mol Biol* 1048: 135-144, 2013.
32. Choung YH, Taura A, Pak K, Choi SJ, Masuda M and Ryan AF: Generation of highly-reactive oxygen species is closely related to hair cell damage in rat organ of Corti treated with gentamicin. *Neuroscience* 161: 214-226, 2009.
33. Zhou M, Sun G, Zhang L, Zhang G, Yang Q, Yin H, Li H, Liu W, Bai X, Li J, *et al*: STK33 alleviates gentamicin-induced ototoxicity in cochlear hair cells and House Ear Institute-Organ of Corti 1 cells. *J Cell Mol Med* 22: 5286-5299, 2018.
34. Mishina NM, Bogdanova YA, Ermakova YG, Panova AS, Kotova DA, Bilan DS, Steinhorn B, Arnér ESJ, Michel T and Belousov VV: Which Antioxidant System Shapes Intracellular H₂O₂ Gradients? *Antioxid Redox Signal* 31: 664-670, 2019.
35. Qi X, Davis B, Chiang YH, Filichia E, Barnett A, Greig NH, Hoffer B and Luo Y: Dopaminergic neuron-specific deletion of p53 gene is neuroprotective in an experimental Parkinson's disease model. *J Neurochem* 138: 746-757, 2016.
36. Zhao H, Yenari MA, Cheng D, Sapolsky RM and Steinberg GK: Bcl-2 overexpression protects against neuron loss within the ischemic margin following experimental stroke and inhibits cytochrome *c* translocation and caspase-3 activity. *J Neurochem* 85: 1026-1036, 2003.
37. Xing ZH, Ma YC, Li XP, Zhang B and Zhang MD: Research progress of puerarin and its derivatives on anti-inflammatory and anti-gout activities. *Zhongguo Zhongyao Zazhi* 42: 3703-3708, 2017 (In Chinese).



This work is licensed under a Creative Commons Attribution-NonCommercial-NoDerivatives 4.0 International (CC BY-NC-ND 4.0) License.